

SEARCHING FOR THE HIGHEST REDSHIFT SOURCES IN 250–500 μm SUBMILLIMETER SURVEYS

ALEXANDRA POPE^{1,3} AND RANGA-RAM CHARY²

¹ National Optical Astronomy Observatory, 950 North Cherry Avenue, Tucson, AZ 85719, USA; pope@noao.edu

² Spitzer Science Center, California Institute of Technology, Pasadena, CA 91125, USA

Received 2010 January 27; accepted 2010 May 3; published 2010 May 13

ABSTRACT

We explore a technique for identifying the highest redshift ($z > 4$) sources in *Herschel*/SPIRE and BLAST submillimeter surveys by localizing the position of the far-infrared dust peak. Just as *Spitzer*/IRAC was used to identify stellar “bump” sources, the far-IR peak is also a redshift indicator; although the latter also depends on the average dust temperature. We demonstrate the wide range of allowable redshifts for a reasonable range of dust temperatures and show that it is impossible to constraint the redshift of individual objects using solely the position of the far-IR peak. By fitting spectral energy distribution models to simulated *Herschel*/SPIRE photometry we show the utility of radio and/or far-infrared data in breaking this degeneracy. With prior knowledge of the dust temperature distribution it is possible to obtain statistical samples of high redshift submillimeter galaxy (SMG) candidates. We apply this technique to the BLAST survey of ECDFS to constrain the number of dusty galaxies at $z > 4$. We find 8 ± 2 galaxies with flux density ratios of $S_{500} > S_{350}$; this sets an upper limit of $17 \pm 4 \text{ deg}^{-2}$ if we assume all are at $z > 4$. This is $< 35\%$ of all 500 μm -selected galaxies down to $S_{500} > 45 \text{ mJy}$ ($L_{\text{IR}} > 2 \times 10^{13} L_{\odot}$ for $z > 4$). Modeling with conventional temperature and redshift distributions estimates the percentage of these 500 μm peak galaxies at $z > 4$ to be between 10% and 85%. Our results are consistent with other estimates of the number density of very high redshift SMGs and follow the decline in the star formation rate density at $z > 4$.

Key words: galaxies: evolution – galaxies: high-redshift – galaxies: starburst – infrared: galaxies – submillimeter: general – techniques: photometric

1. INTRODUCTION

The prevalence of dusty, infrared luminous galaxies at early times tests our theories about early galaxy formation and the production of metals. Semianalytic models predict very small numbers of submillimeter galaxies (SMGs) at extreme redshifts ($z > 4$; e.g., Baugh et al. 2005), and the best observational constraints on the redshift distribution of SMGs are consistent with this (Chapman et al. 2005; Swinbank et al. 2008). Much attention has been paid to recent studies which have spectroscopically confirmed a small number of SMGs at $z > 4$ (Capak et al. 2008; Coppin et al. 2009; Daddi et al. 2009a, 2009b; Knudsen et al. 2010); however, these sources are still only a small fraction of the submillimeter population. Small number statistics and cosmic variance in current submillimeter surveys prohibit an accurate measure of the space density of the most distant SMGs.

The question of the prominence of the high-redshift tail of dusty SMGs can be addressed with imminent submillimeter wide area surveys such as those with the *Herschel Space Observatory* (Pilbratt 2001), the SCUBA-2 camera on the James Clerk Maxwell telescope (JCMT; Holland et al. 2006), and the AzTEC camera on the Large Millimeter Telescope (LMT; Wilson et al. 2008). The *Herschel Space Observatory* is currently collecting data from 70–500 μm over wide survey fields. With an aperture of 3.5 m, *Herschel* is only sensitive to ultra-luminous infrared galaxies (ULIRGs; $L_{\text{IR}} > 10^{12} L_{\odot}$) above $z > 2$ at 250–500 μm before it reaches the confusion limit. One advantage of SPIRE surveys is the simultaneous observations at three wavelengths 250, 350, and 500 μm , which samples the peak of the far-IR spectral energy distribution (SED) due to dust emission in high-redshift galaxies. With prior knowledge of the dust properties which describe the shape of the

SED, the position of the far-IR peak is sensitive to the redshift of the galaxy.

In this Letter, we discuss the power and limitations of using the far-IR peak as a redshift indicator in submillimeter surveys. We apply this technique to the current BLAST survey of the Extended Chandra Deep Field South (ECDFS) and place an upper limit on the number density of 500 μm -selected SMGs at $z > 4$.

Throughout this Letter, we assume a standard cosmology with $H_0 = 71 \text{ km s}^{-1} \text{ Mpc}^{-1}$, $\Omega_M = 0.27$, and $\Omega_{\Lambda} = 0.73$.

2. FAR-IR “BUMP” TECHNIQUE

The 1.6 μm bump in the near-infrared SED of galaxies arises due to a minimum in the H^- opacity in the spectra of cool stars. This bump has been used in extragalactic *Spitzer*/IRAC surveys to identify sources in a specific redshift range (e.g., Wright et al. 1994; Sawicki 2002; Farrah et al. 2008). A similar, but factor of ~ 2 – 3 broader, peak exists in the SED of galaxies at far-IR wavelengths which is caused by the integrated thermal emission from dust of different temperatures. This SED is often parameterized as a blackbody distribution of a particular far-infrared color temperature (T_{dust}) with an additional term to account for the dust emissivity⁴ (e.g., Blain et al. 2002).

The challenge with using the far-IR bump as a redshift indicator is that the average dust temperature and the redshift are degenerate (e.g., Blain 1999; Blain et al. 2003). Wien’s displacement law tells us that the wavelength of the peak of a blackbody scales with the dust temperature. Coupling this with the displacement of the peak due to redshift we find that the observed wavelength of the far-IR peak depends linearly on both the redshift and the inverse of the dust temperature: $\lambda_{\text{obs}}^{\text{max}} \propto (1+z)/T_{\text{dust}}$.

³ *Spitzer* Fellow.

⁴ In this Letter, we assume a dust emissivity, $\beta = 1.5$. The choice of emissivity affects the derived color temperature.

Table 1
Catalog of All Candidate 500 μm “Peaker” Sources

| ID | S_{500} (mJy) | S_{350} (mJy) | S_{250} (mJy) | Field |
|---------------------|--------------------|--------------------|--------------------|-------|
| BLASTJ033311-275611 | 56 ± 14 | <45 | <60 | E |
| BLASTJ033129-275548 | 53 ± 14 | <45 | <60 | E |
| BLASTJ033215-275030 | 50 ± 14 | <45 | <60 | EG |
| BLASTJ033254-273303 | 50 ± 14 | <45 | <60 | |
| BLASTJ033346-274217 | 50 ± 14 | <45 | <60 | |
| BLASTJ033256-280105 | 48 ± 14 | <45 | <60 | E |
| BLASTJ033159-273515 | 47 ± 14 | <45 | <60 | |
| BLASTJ033317-274926 | 46 ± 14 | <45 | <60 | E |

Notes. IDs and fluxes come from Chapin et al. (2010); the uncertainties listed here include both instrument and confusion noise (σ_{tot}). The confusion noise is assumed to be 12, 13, and 15 mJy at 500, 350, and 250 μm , respectively (Chapin et al. 2010). Upper limits correspond to the flux where the catalogs are 90% complete which is equivalent to roughly $3\sigma_{\text{tot}}$. The Field column indicates if the source is within the ECDFS (E) and/or the GOODS-S (G) areas.

The most luminous galaxies in the local universe show far-infrared color temperatures that peak at ~ 40 K, although there is a significant scatter in luminosity–temperature parameter space (e.g., Dunne et al. 2000). For a reasonable range of dust temperatures for ULIRGs, sources that peak at 500 μm can be found anywhere between $z \sim 3$ –6. This is a very large range in redshift, and without prior information about the dust temperature it is difficult to further constrain the redshift with the SPIRE data alone.

3. HIGH-REDSHIFT CANDIDATES IN THE ECDFS BLAST SURVEY

In order to test this technique on observations, we use the data from the BLAST survey of ECDFS (Devlin et al. 2009). BLAST has the same three detectors as *Herschel*/SPIRE but with beam sizes that are twice as big: 36, 42, 60 arcsec FWHM at 250, 350, and 500 μm , respectively (Marsden et al. 2009). We use the publicly released BLAST maps⁵ and the matched filter catalogs (Chapin et al. 2010). These matched filter catalogs do a much better job at de-blending adjacent sources and result in higher signal-to-noise ratios than previous BLAST catalogs (see Chapin et al. 2010 for further details). We restrict our analysis to the central 0.47 deg² of the BLAST image where $\sigma_{\text{inst}} < 10$ mJy at 500 μm . We have conservatively added the confusion noise in quadrature with the instrument noise ($\sigma_{\text{conf}}^2 + \sigma_{\text{inst}}^2 = \sigma_{\text{tot}}^2$) for all analysis in this Letter. We only consider detections if they are $>5\sigma_{\text{inst}}$ ($>3\sigma_{\text{tot}}$). In this central region, there are 23 galaxies robustly detected at 500 μm with $S_{500} > 45$ mJy. We match the 500 μm -selected galaxies to the matched filter catalogs at 250 μm and 350 μm ; we consider any $>5\sigma_{\text{inst}}$ detection within a radius of 60 arcsec to be the counterpart to the 500 μm emission. For sources which are undetected at these other wavelengths, we set upper limits on the 350 and 250 μm fluxes from the 90% completeness limits of the survey (Chapin et al. 2010) which is equivalent to $3\sigma_{\text{tot}}$.

Of these 23 500 μm -selected galaxies, 8 have $S_{500} > S_{350}$ indicating that the dust SED peaks at or near 500 μm —we refer to these galaxies as 500 μm “peakers” (although their peak may be at even longer wavelengths). Interestingly, none of these 500 μm peakers (detected at $>5\sigma_{\text{inst}}$) are detected above $5\sigma_{\text{inst}}$ at 250 and 350 μm . We inspected all of these candidates by hand in the BLAST images to make sure they are not obviously blended.

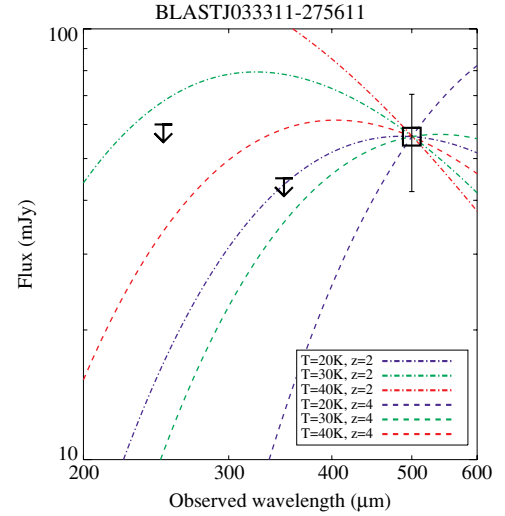


Figure 1. Example far-IR SED of one of our high-redshift candidates from the BLAST ECDFS survey. The current data and limits are consistent with very cold $z \sim 2$ sources as well as $z \sim 4$ sources with average dust temperatures. Stronger limits at 250 and 350 μm will be required to alleviate this degeneracy.

We have not attempted to correct for flux boosting (e.g., Coppin et al. 2006) in this analysis but, since we are not interested in the absolute fluxes and only the relative colors, this is less of a concern. In addition, by considering only higher signal-to-noise ratio sources we ensure that this effect is minimal. In order to assess how photometric uncertainties (from both confusion and instrument noise) affect the number of 500 μm peakers identified, we ran a Monte Carlo simulation to randomly sample the fluxes of each of the 23 sources from a Gaussian distribution $S \pm \sigma_{\text{tot}}$. We find that photometric uncertainties can vary the number of sources with $S_{500} > S_{350}$ by 2. Thus our final number of 500 μm peakers is 8 ± 2 .

These eight high-redshift candidates are listed in Table 1 along with their fluxes, and Figure 1 shows an example SED for one source. Five of these 500 μm peakers are within the ECDFS field and one is within the smaller GOODS-S region (see Table 1). The source within GOODS-S is associated (6 arcsec away) with an AzTEC 1.1 mm detected source (GS11; Scott et al. 2010); however, flux boosting in the BLAST bands prohibits a detailed comparison.

Knowing that a source peaks at (or near) 500 μm does not provide a definitive redshift due to the degeneracy between redshift and temperature (e.g., Figure 2). If we conservatively assume that all 500 μm peakers are at $z > 4$, we can obtain an upper limit on the number density of $z > 4$ galaxies predicted in *Herschel* SPIRE surveys. Based on our analysis of the BLAST data, the number density of galaxies (with $S_{500} > 45$ mJy) which peak at 500 μm is 17 ± 4 deg⁻². We expect that some of these 500 μm peakers will be at $z < 4$ since Figure 2 shows that sources cooler than 40 K can have $S_{500} > S_{350}$ but be at $z < 4$.

To get an estimate of the contamination of low-redshift, cooler galaxies in the 500 μm peaker sample, we must assume a redshift and dust temperature distribution. Assuming a flat redshift distribution⁶ and a dust color temperature distribution of 35 ± 7 K,⁷ we estimate that 15 % of 500 μm peakers will be

⁶ A flat redshift distribution has an equal number of objects per redshift interval (constant dn/dz). This is roughly equivalent to a non-evolving luminosity function at $z > 2$.

⁷ This dust temperature distribution is consistent with local ULIRGs (Dunne et al. 2000) as well as $z \sim 2$ SMGs (Chapman et al. 2005; Pope et al. 2006).

⁵ <http://blastexperiment.info/results.php>

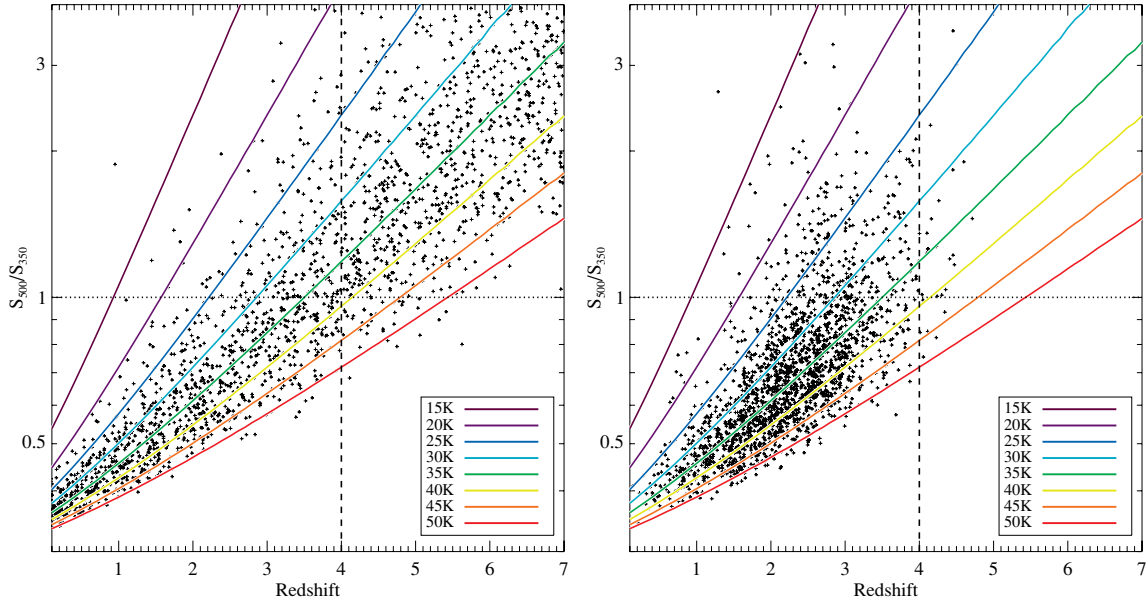


Figure 2. Criteria for selecting 500 μm peakers and the degeneracy between dust temperature and redshift. The curves show the S_{500}/S_{350} flux density ratio of an SED (single temperature modified blackbody with $\beta = 1.5$) for a given T_{dust} (see color legend) as a function of redshift. The horizontal dotted line shows the criteria used to define a source that peaks at 500 μm ; there is a range of redshift and dust temperature combinations that produces this ratio. The data points show a Monte Carlo simulation of 2000 galaxies following a dust temperature distribution of 35 ± 7 K, and a uniform redshift distribution (left panel) or $z = 2.2 \pm 0.8$ (right panel). The uniform redshift distribution results in the majority of 500 μm peakers being at $z > 4$, whereas the Gaussian redshift distribution puts very few sources above $z = 4$ and the majority of 500 μm peakers at $z < 4$.

$z < 4$ (left panel of Figure 2). In addition, we must also account for the contribution from warmer sources at $z > 4$ but which peak at lower wavelengths ($S_{500} < S_{350}$). Assuming a sample of sources at $z > 4$ again following a dust temperature distribution of 35 ± 7 K, we find that only 10 % have $S_{500} < S_{350}$. These two factors roughly cancel each other, and we are left with a constraint on the number density of $z > 4$ sources (with $S_{500} > 45$ mJy) of $< 17 \text{ deg}^{-2}$.

The above limit on the number density of $z > 4$ SMGs ambitiously assumes a flat redshift distribution. If instead we assume the observed redshift distribution of SMGs (2.2 ± 0.8 ; Chapman et al. 2005; Pope et al. 2006), we find only 10% of the 500 μm peakers at $z > 4$ (right panel of Figure 2) which brings the number density estimate down to 2 deg^{-2} . Based on our analysis of the BLAST data, we conclude that the number density of $S_{500} > 45$ mJy sources at $z > 4$ is $< 17 \text{ deg}^{-2}$ and could be as low as 2 deg^{-2} .

With some assumptions about the dust temperature distribution, we have shown that the submillimeter color selection, $S_{500} > S_{350}$, is a plausible way to identify samples containing the highest redshift SMGs selected at these wavelengths (albeit these samples contain contamination from lower redshift objects). Without further multi-wavelength data, it is impossible to tell individually which of the eight candidates are at $z > 4$ and which are just peaking at 500 μm because they have cooler dust temperatures. One way to test the reality of these high-redshift candidates is to further constrain their SEDs with data at longer submillimeter wavelengths such as those from the 870 μm LABOCA survey of ECDFS (Weiß et al. 2009). In order to make a robust comparison between the LABOCA and BLAST fluxes, a correction for flux boosting needs to be applied to both surveys using the same method (e.g., Coppin et al. 2006). This is beyond the scope of this Letter but should be possible with full access to the signal and noise maps from both surveys. Another potential way to break the degeneracy between redshift and temperature for these candidates is with the radio and/or

far-IR (e.g., 100 μm) flux; we discuss this further in the next section.

4. USING RADIO AND FAR-IR DATA TO BREAK THE z - T DEGENERACY

Photometry from 250–500 μm alone can provide an accurate measure of $(1 + z)/T_{\text{dust}}$. Figure 3 shows a simulation of *Herschel* SPIRE photometry for a source that peaks at 500 μm . Fitting modified blackbody models to this data we find the pairs of T and z that fit these data (panel (b) of Figure 3) and the resulting L_{FIR} (panel (c) of Figure 3).

The radio emission from galaxies is known to correlate well with the infrared emission in the local universe (Condon 1992). Because of this radio-infrared correlation, radio data are often used to help identify counterparts to SMGs (e.g., Ivison et al. 2002) and to constrain the redshift (e.g., Carilli & Yun 1999; Hughes et al. 2002; Aretxaga et al. 2007). We demonstrate the latter point in panel (d) of Figure 3. Here, we assume the average value and scatter in the q parameter from fitting local galaxies (Yun et al. 2001). The radio flux is not degenerate with the redshift; however, unfortunately, the large scatter in the local radio-IR correlation provides fairly loose constraints on the redshift of individual objects from the radio flux. Nevertheless, a large fraction of the bright SMGs detected with SPIRE will be above the flux limits of deep ($\sigma_{\text{radio}} < 5 \mu\text{Jy}$) 1.4 GHz radio surveys. With large statistical samples, the redshift distribution inferred from including radio observations should be robust, assuming the radio-IR correlation holds out to high redshift.

Below $\sim 50 \mu\text{m}$ rest frame, the SED of galaxies is no longer dominated by the single temperature-modified blackbody but instead by warmer dust components. This can be seen in panel (a) of Figure 3 where the dash-dotted curve is a Chary & Elbaz (2001, CE01) template representative of local star-forming galaxies. Fitting the CE01 templates (allowing the luminosity and temperature to vary) to the simulated SPIRE photometry

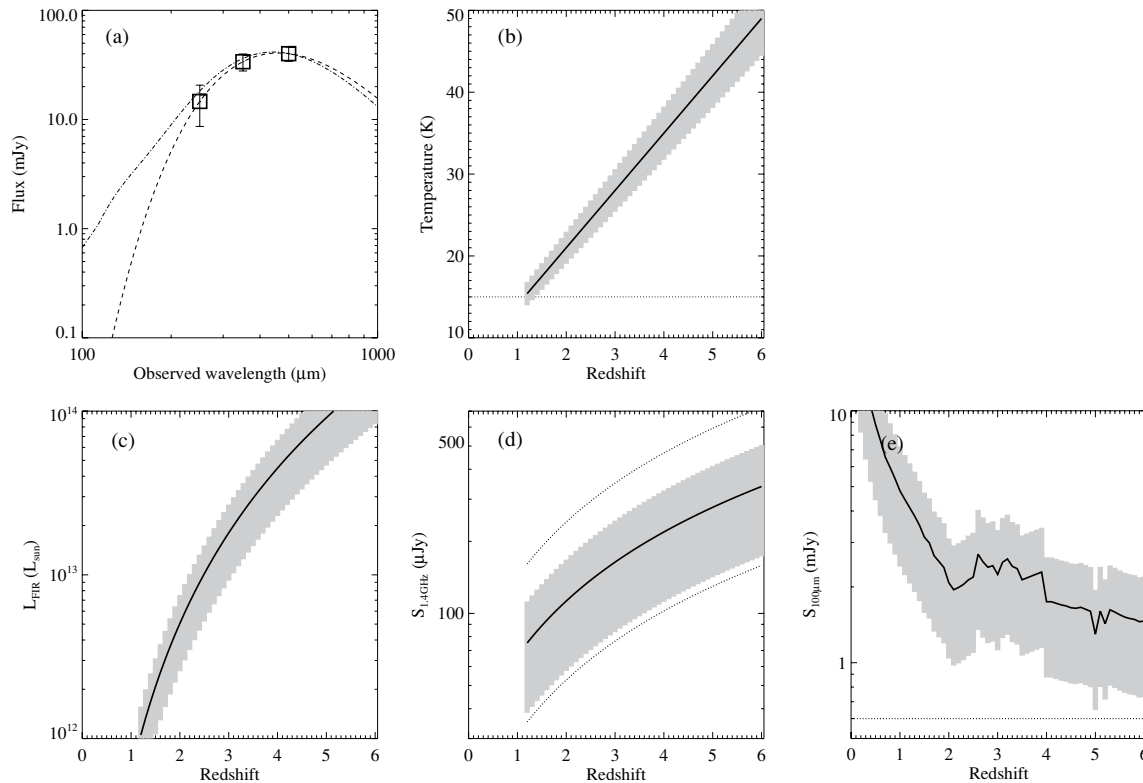


Figure 3. Example of degeneracy in single temperature-modified blackbody SED fitting. (a) Simulated SPIRE photometry of a $500\,\mu\text{m}$ peaker ($S_{500} = 40\,\text{mJy}$). Flux uncertainty includes both confusion ($\sigma_{\text{conf}} \sim 6\,\text{mJy}$) and instrument ($\sigma_{\text{inst}} \sim 1\,\text{mJy}$) noise (the shaded regions in (b)–(e) reflect the errors due to this measurement uncertainty). The dashed curve is the best-fit modified blackbody where temperature and redshift combinations can be anything along the line shown in (b). We have excluded temperatures below 15 K since these are unphysical due to heating by the cosmic microwave background. (c) The resulting L_{FIR} of the best-fit modified blackbody model as a function of redshift. (d) The predicted radio flux of the best-fit modified blackbody model as a function of redshift (solid curve). The dotted curves illustrate the uncertainty resulting from the scatter in the local radio-IR correlation. The dash-dotted curve in (a) is a CE01 template which shows how the true SEDs of galaxies diverge from a single temperature modified blackbody at wavelengths shorter than around $50\,\mu\text{m}$ in the rest frame. (e) Estimated $100\,\mu\text{m}$ flux for the best-fit CE01 SED as a function of redshift. The dot-dashed curve shows the 5σ depth of the deepest PACS extragalactic survey, GOODS *Herschel* (PI: D. Elbaz). Deep radio and PACS observations can help break the degeneracy between redshift and dust temperature for the most luminous dusty galaxies.

we estimate the $100\,\mu\text{m}$ flux as a function of redshift (panel (e) of Figure 3). While the curve is not smooth (due to discrete templates within the CE01 library), overall the far-IR flux can constrain the redshift for this simulated galaxy with no prior assumption on its dust temperature. The dotted line in panel (e) of Figure 3 shows the sensitivity of the deepest *Herschel* PACS extragalactic survey (GOODS *Herschel*, PI: D. Elbaz); this deep survey should detect bright SMGs beyond $z \sim 3$ by measuring the redshifted emission from warm dust that is heated in O&B star-forming regions and appears to correlate well with ongoing star formation (Calzetti et al. 2005).

5. DISCUSSION

From the BLAST ECDFS data we estimate a space density of $<17\,\text{deg}^{-2}$ for sources with $S_{500} > 45\,\text{mJy}$ at $z > 4$; this is $<35\%$ (8/23) of all sources selected down to these depths in the BLAST data. These bright $500\,\mu\text{m}$ -selected SMGs at $z > 4$ contribute $<1\%$ of the total background emission at $500\,\mu\text{m}$ (Fixsen et al. 1998).

Constrained by a recent analysis of the infrared extragalactic background light (EBL), galaxies evolution models predict the source density of galaxies with $S_{500} > 27\,\text{mJy}$ ⁸ at $z > 4$ to be $1\text{--}5\,\text{deg}^{-2}$ (Chary & Pope 2010). The range of predicted

number density comes from considering two evolutions of the models both of which fit the observed EBL. We find that our current observational constraint is consistent with both evolutionary scenarios. Future submillimeter surveys with much larger telescopes such as JCMT, LMT, and CCAT will reach much deeper flux limits before hitting the confusion limit. With these surveys, we can expect to detect many more dusty galaxies at $z > 4$; the models in Chary & Pope (2010) predict a number density of $40\text{--}200\,\text{deg}^{-2}$ at $z > 4$ for galaxies down to $5\,\text{mJy}$ at $500\,\mu\text{m}$.

In the past two years, the tally of $z > 4$ spectroscopically confirmed SMGs has grown from zero to five⁹ (Capak et al. 2008; Coppin et al. 2009; Daddi et al. 2009a, 2009b). Coppin et al. (2009) estimate the number density of SMGs at $z > 4$ by combining these five sources from three independent submillimeter surveys and find a lower limit of $>7\,\text{deg}^{-2}$. While this is consistent with our predictions for $500\,\mu\text{m}$ -selected galaxies, we note that the sensitivities of the BLAST and submillimeter surveys are not the same at $z = 4$; only 1/5 of the $z > 4$ spectroscopically confirmed SMGs might be detected down to the BLAST ECDFS survey depths (assuming a typical SMG dust temperature). Folding this in the Coppin et al. (2009) estimate down to $S_{850} > 20\,\text{mJy}$ scales to $>1.4\,\text{deg}^{-2}$ at $z > 4$.

There is some evidence that large numbers of very massive galaxies at $z > 4$ pose a substantial challenge to standard galaxy

⁸ In order to compare to the models, we need to assume a rough correction for flux boosting of the BLAST measurements. Based on Eales et al. (2009), we adopt an average correction of 0.6 to the BLAST fluxes which effectively brings the flux limit down to $27\,\text{mJy}$.

⁹ A sixth $z > 4$ SMG recently appeared in the literature (Knudsen et al. 2010).

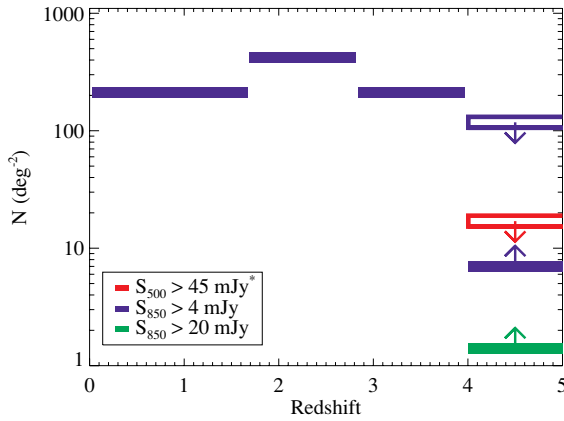


Figure 4. Histogram showing the number density of submillimeter-selected galaxies as a function of redshift. Our new upper limit from the 500 μm BLAST analysis is shown as the open red bar. The blue and green bars are estimates for SCUBA 850 μm -selected galaxies from the literature where filled bars denote spectroscopic samples ($z < 4$, Chapman et al. 2005; $z > 4$, Coppin et al. 2009), and open bars denote photometric redshift samples (Pope et al. 2006). *Note that the BLAST sample has not been corrected for flux boosting, completeness, or spurious sources. The combination of these effects will act to decrease the true flux limit of this sample.

formation theory (e.g., Baugh et al. 2005). Figure 4 summarizes the current observational constraints on the number density of bright SMGs as a function of redshift. Blue and green bars are for 850 μm -selected SMGs using values from the literature (Chapman et al. 2005; Coppin et al. 2009; Pope et al. 2006) and the red bar is our new upper limit from the analysis in this Letter of the BLAST 500 μm -selected sources. Overall, there appears no room for a large fraction of the SMG population to be above $z = 4$ down to these flux limits.

6. SUMMARY

We have shown that the degeneracy between dust temperature and redshift severely limits the use of the far-IR dust peak alone as a redshift indicator. The color selection of $S_{500} > S_{350}$ (and $S_{500} > S_{250}$) can be used to identify samples of candidate high-redshift galaxies. Further constraining the redshift of individual sources requires prior knowledge of the dust temperature or additional multi-wavelength data, particularly in the radio or at 100 μm .

We present eight candidate 500 μm “peakers” from the BLAST ECDFS survey with $S_{500} > 45$ mJy; a fraction of which we expect to be at $z > 4$ depending on the distribution of dust temperatures. The number density of these high-redshift candidates is $< 17 \text{ deg}^{-2}$ and is consistent with the number densities of the brightest 850 μm -selected galaxies. The corresponding fraction of 500 μm -selected galaxies in the BLAST survey which could be at $z > 4$ is $< 35\%$.

To further constrain the space density of the most distant SMGs will require deep, wide area surveys with *Herschel*/

SPIRE in addition to sufficiently deep multi-wavelength data to weed out the genuine high-redshift candidates from 500 μm “peakers” that are lower redshift galaxies with cooler than average dust temperatures. Regardless, our upper limits on the number density of $z > 4$ luminous dusty galaxies suggest a strong decline in their number density from $z \sim 2$.

We thank the referee for constructive comments which improved the presentation of this work. We thank the BLAST team for making their data public. A.P. acknowledges support provided by NASA through the *Spitzer Space Telescope* Fellowship Program, through a contract issued by the Jet Propulsion Laboratory, California Institute of Technology under a contract with NASA.

REFERENCES

- Aretxaga, I., et al. 2007, *MNRAS*, **379**, 1571
 Baugh, C. M., Lacey, C. G., Frenk, C. S., Granato, G. L., Silva, L., Bressan, A., Benson, A. J., & Cole, S. 2005, *MNRAS*, **356**, 1191
 Blain, A. W. 1999, *MNRAS*, **309**, 955
 Blain, A. W., Barnard, V. E., & Chapman, S. C. 2003, *MNRAS*, **338**, 733
 Blain, A. W., Smail, I., Ivison, R. J., Kneib, J.-P., & Frayer, D. T. 2002, *Phys. Rep.*, **369**, 111
 Calzetti, D., et al. 2005, *ApJ*, **633**, 871
 Capak, P., et al. 2008, *ApJ*, **681**, L53
 Carilli, C. L., & Yun, M. S. 1999, *ApJ*, **513**, L13
 Chapin, E. L., et al. 2010, *MNRAS*, submitted (arXiv:1003.2647)
 Chapman, S. C., Blain, A. W., Smail, I., & Ivison, R. J. 2005, *ApJ*, **622**, 772
 Chary, R., & Elbaz, D. 2001, *ApJ*, **556**, 562
 Chary, R., & Pope, A. 2010, *ApJ*, submitted (arXiv:1003.1731)
 Condon, J. J. 1992, *ARA&A*, **30**, 575
 Coppin, K., et al. 2006, *MNRAS*, **372**, 1621
 Coppin, K. E. K., et al. 2009, *MNRAS*, **395**, 1905
 Daddi, E., Dannerbauer, H., Krips, M., Walter, F., Dickinson, M., Elbaz, D., & Morrison, G. E. 2009a, *ApJ*, **695**, L176
 Daddi, E., et al. 2009b, *ApJ*, **694**, 1517
 Devlin, M. J., et al. 2009, *Nature*, **458**, 737
 Dunne, L., Eales, S., Edmunds, M., Ivison, R., Alexander, P., & Clements, D. L. 2000, *MNRAS*, **315**, 115
 Eales, S., et al. 2009, *ApJ*, **707**, 1779
 Farrah, D., et al. 2008, *ApJ*, **677**, 957
 Fixsen, D. J., Dwek, E., Mather, J. C., Bennett, C. L., & Shafer, R. A. 1998, *ApJ*, **508**, 123
 Holland, W. S., et al. 2006, *Proc. SPIE*, **6275**, 45
 Hughes, D. H., et al. 2002, *MNRAS*, **335**, 871
 Ivison, R. J., et al. 2002, *MNRAS*, **337**, 1
 Knudsen, K. K., Kneib, J.-P., Richard, J., Petitpas, G., & Egami, E. 2010, *ApJ*, **709**, 210
 Marsden, G., et al. 2009, *ApJ*, **707**, 1729
 Pilbratt, G. L. 2001, in *The Promise of the Herschel Space Observatory*, ed. G. L. Pilbratt et al. (ESA-SP 460; Noordwijk: ESA), **13**
 Pope, A., et al. 2006, *MNRAS*, **370**, 1185
 Sawicki, M. 2002, *AJ*, **124**, 3050
 Scott, K. S., et al. 2010, *MNRAS*, in press (arXiv:1003.1768)
 Swinbank, A. M., et al. 2008, *MNRAS*, **391**, 420
 Weiß, A., et al. 2009, *ApJ*, **707**, 1201
 Wilson, G. W., et al. 2008, *MNRAS*, **386**, 807
 Wright, E. L., Eisenhardt, P., & Fazio, G. 1994, *BAAS*, **26**, 893
 Yun, M. S., Reddy, N. A., & Condon, J. J. 2001, *ApJ*, **554**, 803